



ELSEVIER

Available online at [www.sciencedirect.com](http://www.sciencedirect.com)

SCIENCE @ DIRECT®

PHYSICS LETTERS B

Physics Letters B 584 (2004) 233–240

[www.elsevier.com/locate/physletb](http://www.elsevier.com/locate/physletb)

## Formation of hot heavy nuclei in supernova explosions

A.S. Botvina<sup>a,b</sup>, I.N. Mishustin<sup>c,d,e</sup>

<sup>a</sup> Cyclotron Institute, Texas A&M University, College Station, TX 77843, USA

<sup>b</sup> Institute for Nuclear Research, 117312 Moscow, Russia

<sup>c</sup> Institut für Theoretische Physik, Goethe Universität, D-60054 Frankfurt am Main, Germany

<sup>d</sup> Niels Bohr Institute, DK-2100 Copenhagen, Denmark

<sup>e</sup> Kurchatov Institute, RRC, 123182 Moscow, Russia

Received 30 December 2003; accepted 23 January 2004

Editor: P.V. Landshoff

### Abstract

We point out that during the supernova II type explosion the thermodynamical conditions of stellar matter between the proton-neutron star and the shock front correspond to the nuclear liquid–gas coexistence region, which can be investigated in nuclear multifragmentation reactions. We have demonstrated, that neutron-rich hot heavy nuclei can be produced in this region. The production of these nuclei may influence dynamics of the explosion and contribute to the synthesis of heavy elements.

© 2004 Elsevier B.V. All rights reserved. Open access under [CC BY license](https://creativecommons.org/licenses/by/4.0/).

PACS: 25.70.Pq; 26.50.+x; 26.30.+k; 21.65.+f

In recent years significant progress has been made by nuclear community in understanding properties of highly excited nuclear systems. Such systems are routinely produced now in nuclear reactions induced by hadrons and heavy ions of various energies. Under certain conditions, which are well studied experimentally, the intermediate nuclear system is produced in a state close to statistical equilibrium. At low excitation energies this is nothing but a well-known compound nucleus. At excitation energies exceeding 3 MeV per nucleon the intermediate system first expands and then splits into an ensemble of hot nuclear fragments (multifragmentation). At excitation energies above 10 MeV per nucleon the equilibrated system is composed of

nucleons and lightest clusters (vaporisation). These different intermediate states can be understood as a manifestation of the liquid–gas type phase transition in finite nuclear systems [1]. A very good description of such systems is obtained within the framework of statistical multifragmentation model (SMM) [2].

According to present understanding, based on numerous theoretical and experimental studies of multifragmentation reactions, prior to the break-up a transient state of nuclear matter is formed, where hot nuclear fragments exist in equilibrium with free nucleons. This state is characterized by a certain temperature  $T \sim 3\text{--}6$  MeV and a density which is typically 3–5 times smaller than the nuclear saturation density,  $\rho_0 \approx 0.15 \text{ fm}^{-3}$ . Theoretical calculations [2] show that relatively heavy fragments may survive in the liquid–gas coexistence region. In thermodynamic limit these

*E-mail address:* [botvina@comp.tamu.edu](mailto:botvina@comp.tamu.edu) (A.S. Botvina).

heavy fragments would correspond to the infinite liquid phase [3]. This statistical picture of multifragmentation is confirmed by numerous experimental observations, such as an evolution of the fragment mass distribution with energy (temperature), fragment correlations revealing the critical behavior, anomaly in the caloric curve, and by many others (see, e.g., [2,4–6]). Recent experiments (e.g., [7]) directly confirm that primary fragments are really hot, their internal excitation energy may reach up to 3 MeV per nucleon. Properties of these hot nuclei can be extracted from multifragmentation reactions and used in analyzes of other physical processes, where similar nuclei are expected to be produced.

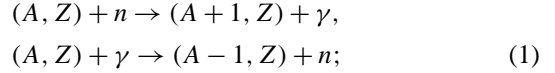
In this Letter we are going to use the knowledge accumulated from multifragmentation studies for better understanding nuclear physics associated with collapse of massive stars and supernova type II explosions. More specifically, we consider the possibility of producing hot heavy nuclei in a protoneutron star, and in hot bubble between the protoneutron star and the shock front [8]. This region is crucial for success (or failure) of the supernova explosion. The presence of hot nuclei will influence many processes. For example, the electron capture on nuclei plays an important role in supernova dynamics [9]. In particular, the electron capture rates are sensitive to the nuclear composition and details of nuclear structure (see, e.g., [10]). The neutrino-induced reactions are very sensitive to the nuclear structure effects and properties of weak interactions in nuclei (see, e.g., [11]). It is also important that the presence of nuclei favors the explosion via the energy balance of matter in the bubble [12].

In the supernova environment, as compared to the nuclear reactions, several new important ingredients should be taken into consideration. First, the matter at stellar scales must be electrically neutral and therefore electrons should be included to balance positive nuclear charge. Second, energetic photons present in hot matter may change nuclear composition via photonuclear reactions. And third, the matter is irradiated by a strong neutrino wind from the protoneutron star. Below we apply a grandcanonical version [13] of the SMM to calculate mass and charge distributions of nuclear species under these conditions.

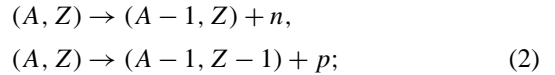
We consider macroscopic volumes of matter consisting of various nuclear species  $(A, Z)$ , nucleons  $(n = (1, 0)$  and  $p = (1, 1))$ , electrons  $(e^-)$  and pos-

itrons  $(e^+)$  under condition of electric neutrality. In supernova matter there exist several reaction types responsible for the chemical composition. At low densities the most important ones are:

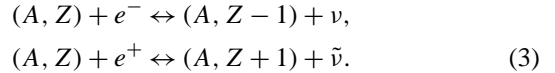
- (1) neutron capture and photodisintegration of nuclei



- (2) neutron and proton emission by hot nuclei



- (3) weak processes induced by electrons/positrons and neutrinos/antineutrinos



The characteristic reaction times for neutron capture, photodisintegration of nuclei and nucleon emission can be written as

$$\begin{aligned} \tau_{\text{cap}} &= [\langle \sigma_{nA} v_{nA} \rangle \rho_n]^{-1}, \\ \tau_{\gamma A} &= [\langle \sigma_{\gamma A} v_{\gamma A} \rangle \rho_\gamma]^{-1}, \\ \tau_{n,p} &= \hbar / \Gamma_{n,p}, \end{aligned}$$

respectively. Here  $\sigma_{nA}$  and  $\sigma_{\gamma A}$  are the corresponding cross sections,  $v_{nA}$  and  $v_{\gamma A}$  are the relative (invariant) velocities, and  $\Gamma_{n,p}$  is the neutron (proton) decay width. Our estimates show that at temperatures and densities of interest these reaction times vary within the range from 10 to  $10^6$  fm/c, that is indeed very short compared to the characteristic hydrodynamic time of a supernova explosion, about 100 ms [8]. The nuclear statistical equilibrium is a reasonable assumption under these conditions. However, one should specify what kind of equilibrium is expected. For densities  $\rho > 10^{-5} \rho_0$  and for the expected temperatures of the environment,  $T \lesssim 5$  MeV, we obtain  $\tau_{\gamma A} \gg \tau_{\text{cap}}, \tau_{n,p}$ , i.e., the photodisintegration is less important than other processes. There exists a range of densities and temperatures, for example,  $\rho \gtrsim 10^{-5} \rho_0$  at  $T = 1$  MeV, and  $\rho \gtrsim 10^{-3} \rho_0$  at  $T = 3$  MeV, where the neutron capture dominates, i.e.,  $\tau_{\text{cap}} < \tau_{n,p}$ . Under these conditions new channels for production and decay of nuclei will appear (e.g., a fast break-up with

emission of  $\alpha$ -particles or heavier clusters) which restore the detailed balance. We expect that in this situation an ensemble of various nuclear species will be generated like in a liquid–gas coexistence region, as observed in the multifragmentation reactions. Here the nuclear system is characterized by the temperature  $T$ , baryon density  $\rho_B$  and electron fraction  $Y_e$  (i.e., the ratio of electron and baryon densities). One may expect that new nuclear effects come into force in this environment. For example, at high temperature the masses and level structure in hot nuclei can be different from those observed in cold nuclei (see, e.g., [14]).

The weak interaction reactions are much slower. The direct and inverse reactions in Eq. (3) involve both free nucleons and all nuclei present in the matter. It is most likely that at early stages of a supernova explosion neutrinos/antineutrinos are trapped inside the neutrinosphere around a protoneutron star [15]. In this case we include the lepton number conservation condition by fixing the lepton fraction  $Y_L$ . Out of the surface of the neutrinosphere one should take into account the continuous neutrino flux propagating through the hot bubble. Due to large uncertainties in the weak interaction rates, below we consider three physically distinctive situations:

- (1) fixed lepton fraction  $Y_L$  corresponding to a  $\beta$ -equilibrium with trapped neutrinos inside the neutrinosphere (early stage);
- (2) fixed electron fraction  $Y_e$  but without  $\beta$ -equilibrium inside a hot bubble (early and intermediate times);
- (3) full  $\beta$ -equilibrium without neutrino (late times, after cooling and neutrino escape).

The second case corresponds to a non-equilibrium situation which may take place in the bubble at early times, before the electron capture becomes efficient.

Chemical potential of a species  $i$  with baryon number  $B_i$ , charge  $Q_i$  and lepton number  $L_i$ , which participates in chemical equilibrium, can be found from the general expression:

$$\mu_i = B_i \mu_B + Q_i \mu_Q + L_i \mu_L, \quad (4)$$

where  $\mu_B$ ,  $\mu_Q$  and  $\mu_L$  are three independent chemical potentials which are determined from the conservation of total baryon number  $B = \sum_i B_i$  electric charge

$Q = \sum_i Q_i$  and lepton number  $L = \sum_i L_i$  of the system. This gives

$$\begin{aligned} \mu_{AZ} &= A \mu_B + Z \mu_Q, \\ \mu_{e^-} &= -\mu_{e^+} = -\mu_Q + \mu_L, \\ \mu_\nu &= -\mu_{\bar{\nu}} = \mu_L. \end{aligned} \quad (5)$$

These relations are also valid for nucleons,  $\mu_n = \mu_B$  and  $\mu_p = \mu_B + \mu_Q$ . If  $\nu$  and  $\bar{\nu}$  escape freely from the system, the lepton number conservation is irrelevant and  $\mu_L = 0$ . In this case two remaining chemical potentials are determined from the conditions of baryon number conservation and electro-neutrality:

$$\begin{aligned} \rho_B &= \frac{B}{V} = \sum_{AZ} A \rho_{AZ}, \\ \rho_Q &= \frac{Q}{V} = \sum_{AZ} Z \rho_{AZ} - \rho_e = 0. \end{aligned}$$

Here  $\rho_e = \rho_{e^-} - \rho_{e^+}$  is the net electron density. The pressure of the relativistic electron–positron gas can be written as

$$\begin{aligned} P_e &= \frac{\mu_e^4}{12\pi^2} \left[ 1 + 2 \left( \frac{\pi T}{\mu_e} \right)^2 + \frac{7}{15} \left( \frac{\pi T}{\mu_e} \right)^4 \right. \\ &\quad \left. - \frac{m_e^2}{\mu_e^2} \left( 3 + \left( \frac{\pi T}{\mu_e} \right)^2 \right) \right], \end{aligned}$$

where first order correction due to the finite electron mass is included. The net number density  $\rho_e$  and entropy density  $s_e$  can be obtained now from standard thermodynamic relations as  $\rho_e = \partial P_e / \partial \mu_e$  and  $s_e = \partial P_e / \partial T$ . Neutrinos are taken into account in the same way, but as massless particles, and with the spin factor twice smaller than the electron one.

For describing an ensemble of nuclear species under supernova conditions one can safely use the grand canonical approximation [2,13]. After integrating out translational degrees of freedom one can write pressure of nuclear species as

$$\begin{aligned} P_{\text{nuc}} &= T \sum_{AZ} g_{AZ} \frac{V_f A^{3/2}}{V \lambda_T^3} \exp \left[ -\frac{1}{T} (F_{AZ} - \mu_{AZ}) \right] \\ &\equiv T \sum_{AZ} \rho_{AZ}, \end{aligned} \quad (6)$$

where  $\rho_{AZ}$  is the density of nuclear species with mass  $A$  and charge  $Z$ . Here  $g_{AZ}$  is the g.-s. degeneracy factor of species  $(A, Z)$ ,  $\lambda_T = (2\pi \hbar^2 / m_N T)^{1/2}$  is

the nucleon thermal wavelength,  $m_N \approx 939$  MeV is the average nucleon mass.  $V$  is the actual volume of the system and  $V_f$  is so-called free volume, which accounts for the finite size of nuclear species. We assume that all nuclei have normal nuclear density  $\rho_0$ , so that the proper volume of a nucleus with mass  $A$  is  $A/\rho_0$ . At low densities the finite-size effect can be included via the excluded volume approximation  $V_f/V \approx (1 - \rho_B/\rho_0)$ .

The internal excitations of nuclear species ( $A, Z$ ) play an important role in regulating their abundance. Sometimes they are included through the population of nuclear levels known for nearly cold nuclei (see, e.g., [16]). However, in the supernova environment not only the excited states but also the binding energies of nuclei will be strongly affected by the surrounding matter. By this reason, we find it more justified to use another approach which can easily be generalized to include in-medium modifications. Namely, the internal free energy of species ( $A, Z$ ) with  $A > 4$  is parameterized in the spirit of the liquid drop model

$$F_{AZ}(T, \rho_e) = F_{AZ}^B + F_{AZ}^S + F_{AZ}^{\text{sym}} + F_{AZ}^C, \quad (7)$$

where the right-hand side contains, respectively, the bulk, the surface, the symmetry and the Coulomb terms. The first three terms are written in the standard form [2],

$$F_{AZ}^B(T) = \left(-w_0 - \frac{T^2}{\varepsilon_0}\right)A, \quad (8)$$

$$F_{AZ}^S(T) = \beta_0 \left(\frac{T_c^2 - T^2}{T_c^2 + T^2}\right)^{5/4} A^{2/3}, \quad (9)$$

$$F_{AZ}^{\text{sym}} = \gamma \frac{(A - 2Z)^2}{A}, \quad (10)$$

where  $w_0 = 16$  MeV,  $\varepsilon_0 = 16$  MeV,  $\beta_0 = 18$  MeV,  $T_c = 18$  MeV and  $\gamma = 25$  MeV are the model parameters which are extracted from nuclear phenomenology and provide a good description of multifragmentation data [2,4–7]. However, these parameters, especially  $\gamma$ , can be different in hot neutron-rich nuclei, and they need more precise determination in nuclear experiments (see discussion, e.g., in [17]). In the Coulomb term we include the modification due to the screening effect of electrons. By using the Wigner–Seitz approx-

imation it can be expressed as [18]

$$F_{AZ}^C(\rho_e) = \frac{3}{5}c(\rho_e)\frac{(eZ)^2}{r_0A^{1/3}},$$

$$c(\rho_e) = \left[1 - \frac{3}{2}\left(\frac{\rho_e}{\rho_{0p}}\right)^{1/3} + \frac{1}{2}\left(\frac{\rho_e}{\rho_{0p}}\right)\right], \quad (11)$$

where  $r_0 = 1.17$  fm and  $\rho_{0p} = (Z/A)\rho_0$  is the proton density inside the nuclei. The screening function  $c(\rho_e)$  is 1 at  $\rho_e = 0$  and 0 at  $\rho_e = \rho_{0p}$ . We want to stress that both the reduction of the surface energy due to the finite temperature and the reduction of the Coulomb energy due to the finite electron density favor the formation of heavy nuclei. Nucleons and light nuclei ( $A \leq 4$ ) are considered as structureless particles characterized only by mass and proper volume.

As follows from Eq. (6), the fate of heavy nuclei depends sensitively on the relationship between  $F_{AZ}$  and  $\mu_{AZ}$ . In order to avoid an exponentially divergent contribution to the baryon density, at least in the thermodynamic limit ( $A \rightarrow \infty$ ), inequality  $F_{AZ} \gtrsim \mu_{AZ}$  must hold. The equality sign here corresponds to the situation when a big nuclear fragment coexists with the gas of smaller clusters [3]. When  $F_{AZ} > \mu_{AZ}$  only small clusters with nearly exponential mass spectrum are present. However, there exist thermodynamic conditions corresponding to  $F_{AZ} \approx \mu_{AZ}$  when the mass distribution of nuclear species is broadest. The advantage of our approach is that we consider all the fragments present in this transition region, contrary to the previous calculations [18,19], which consider only one “average” nucleus characterizing the liquid phase.

Mass distributions and charge-to-mass ratios of nuclear species were obtained for three sets of physical conditions expected in protoneutron stars and in supernova explosions. We take baryon number  $B = 1000$  and perform calculations for all fragments with  $1 \leq A \leq 1000$  and  $0 \leq Z \leq A$  in a box of fixed volume  $V$ . The fragments with larger masses ( $A > 1000$ ) can be produced only at a very high density  $\rho_B \gtrsim 0.5\rho_0$  [12,18], which is appropriate for the regions deep inside the protoneutron star, and which is not considered here. First we consider the case when lepton fraction is fixed as expected inside a neutrinosphere. Fig. 1 shows the results for  $Y_L = 0.4$  and  $Y_L = 0.2$ . For a typical temperature  $T = 3$  MeV we find that the islands of heavy nuclei,  $100 < A < 500$ , can appear only at relatively high baryon density,  $\rho_B = 0.1\rho_0$ . These nu-

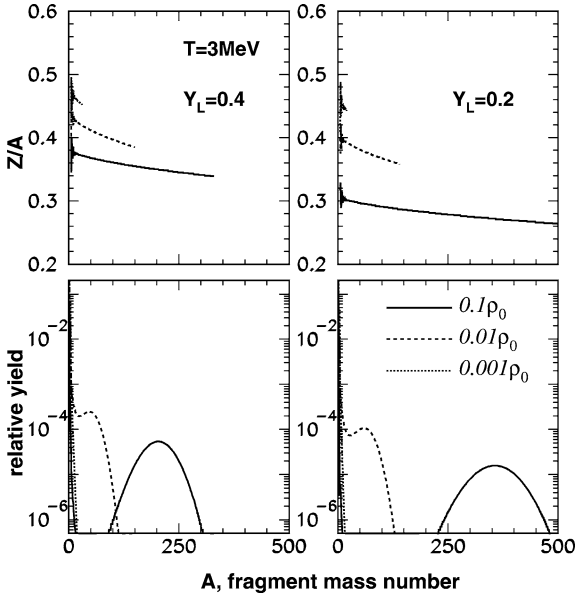


Fig. 1. Mass distributions (bottom panels) and average charge to mass number ratios (top panels) of hot primary fragments produced at temperature  $T = 3$  MeV, and for different densities (in shares of the normal nuclear density  $\rho_0$ ) shown on the figure. The calculations are for the lepton number conservation: the lepton fraction is  $Y_L = 0.4$  on the left panels, and  $Y_L = 0.2$  on the right ones.

clei are neutron-rich:  $Z/A \approx 0.36$  and  $Z/A \approx 0.27$  for  $Y_L = 0.4$  and  $Y_L = 0.2$ , respectively. The  $Z/A$  ratios are decreasing with  $A$  less rapidly than in the nuclear multifragmentation case [20]. This can be explained by the screening effect of electrons. The width of the charge distribution at given  $A$  is determined by  $T$  and  $\gamma$ :  $\sigma_Z \approx \sqrt{AT/8\gamma}$  [13,20]. At lower density,  $\rho_B = 0.01\rho_0$ , the mass distribution is rather flat up to  $A \approx 80$  and then decreases rapidly for larger  $A$ . For  $\rho = 10^{-3}\rho_0$  only light clusters are present and the mass distribution drops exponentially. We have also found that for  $T = 5$  MeV the island of heavy nuclei ( $300 < A < 700$ ) is observed at very high densities,  $\rho_B \approx 0.3\rho_0$ , but at  $\rho_B = 0.1\rho_0$  the mass distribution is very broad, up to  $A \approx 180$ . This picture is similar to the nuclear liquid–gas coexistence region observed in finite systems [2].

Let us consider the situation more appropriate for a hot bubble at early times of a supernova explosion, when the neutrino wind from the core interacts with the infalling matter. In this case only the electron fraction is fixed, and the electron and proton chemical po-

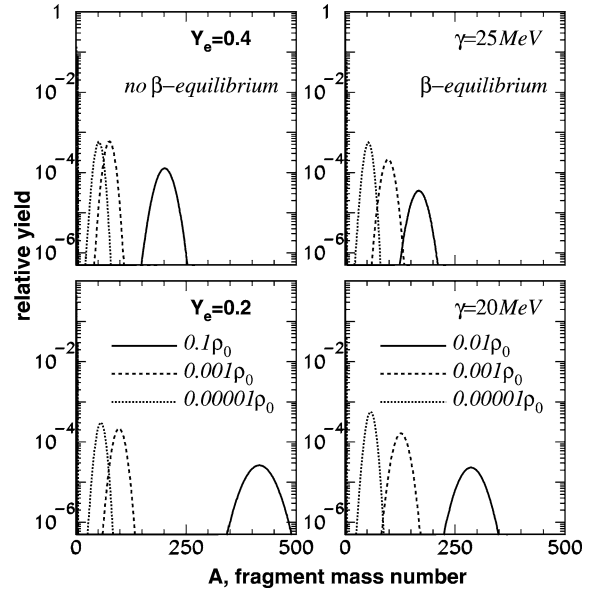


Fig. 2. Mass distributions of hot primary fragments produced at temperature  $T = 1$  MeV, and for different densities. Left panels are for the case of the fixed electron fractions  $Y_e$  (no  $\beta$ -equilibrium); right panels are for the full  $\beta$ -equilibrium (without neutrino capture), and for different symmetry energy coefficients  $\gamma$ .

tentials are determined independently, without using the equilibrium relation  $\mu_e = -\mu_Q$ . Corresponding results for  $Y_e = 0.4$  and  $Y_e = 0.2$  at  $T = 1$  MeV and several baryon densities are presented in Fig. 2 (left top and bottom panels). One can see that heavy nuclei,  $50 < A < 500$ , can be produced in very broad range of densities,  $0.1\rho_0 > \rho_B > 10^{-5}\rho_0$ . At given density the mass distribution has a Gaussian shape. In the  $Y_e = 0.4$  case the most probable nuclei, corresponding to the maxima of distributions, have  $Z/A$  ratios 0.400, 0.406, and 0.439, for densities  $0.1\rho_0$ ,  $10^{-3}\rho_0$ , and  $10^{-5}\rho_0$ , respectively. The Gaussian mass distributions may in some cases justify earlier calculations [18,19], when only one heavy nuclear species was assumed at each density. As seen from the bottom panel, changing the electron fraction from 0.4 to 0.2 leads to a significant increase of nuclear masses. Also, the nuclei become more neutron rich: the corresponding  $Z/A$  ratios are 0.280, 0.359, and 0.420. It is interesting to note that the combination of chemical potentials  $\mu_e + \mu_p - \mu_n$  which drives the electron capture might be quite large in this case. For instance, for  $Y_e = 0.4$  this value is 14 MeV at  $\rho_B = 10^{-3}\rho_0$ , so that the elec-

tron capture rate will be significantly enhanced compared to the equilibrium rate at  $T = 1$  MeV.<sup>1</sup>

In the right panels of Fig. 2 we show results for the case of full  $\beta$ -equilibrium without neutrinos. We observe that the distributions are quite similar to the ones shown in the left panels. For the case of the standard symmetry energy with  $\gamma = 25$  MeV we obtain that the  $Z/A$  ratios of the most probable nuclei are 0.311, 0.359, and 0.435, for densities  $0.01\rho_0$ ,  $10^{-3}\rho_0$ , and  $10^{-5}\rho_0$ , respectively. It is seen from the bottom panel that by slightly decreasing the  $\gamma$ -coefficient in the symmetry energy one can shift mass distributions to higher masses. The nuclei in this case are even more neutron rich, the corresponding  $Z/A$  ratios are 0.241, 0.317, and 0.417. For easier comparison, in left and right panels we present calculations for the baryon densities  $10^{-3}$  and  $10^{-5}\rho_0$ , which are more realistic in the bubble. The comparison shows that in the course of  $\beta$ -equilibration the mass distributions may shift by 10–40 mass units. This shift also characterizes uncertainties in the nuclear composition associated with the electron capture reactions.

Fig. 3 shows the fractions of free electrons and neutrons as a function of baryon density. On the left panels it was calculated for the  $\beta$ -equilibrium neutrinoless matter at  $T = 1$  MeV. These particles, besides heavy nuclei, dominate in the supernova matter. As was realized long ago [12], the electrons are absorbed at large densities because of the high electron chemical potential. In this Letter we point out the importance of free neutrons in the liquid–gas coexistence region for maintaining a high rate of nuclear reactions. A noticeable change in the trend is seen at  $\rho_B \approx 10^{-4}\rho_0$ . At lower density  $Y_n \approx 0.2$  that means that 80% of neutrons are trapped in nuclei. At higher densities more and more neutrons are dripping out of nuclei, and at  $\rho_B > 10^{-3}\rho_0$  more than half of the neutrons are free. This behavior correlates with the decreasing number of electrons and a relatively small share of heavy nuclei in the system. However, at higher densities, the structure of matter changes because of the neutrino/antineutrino and electron/positron capture reactions [12]. The case of lepton conservation is shown on the right panels of Fig. 3. One can see that in this

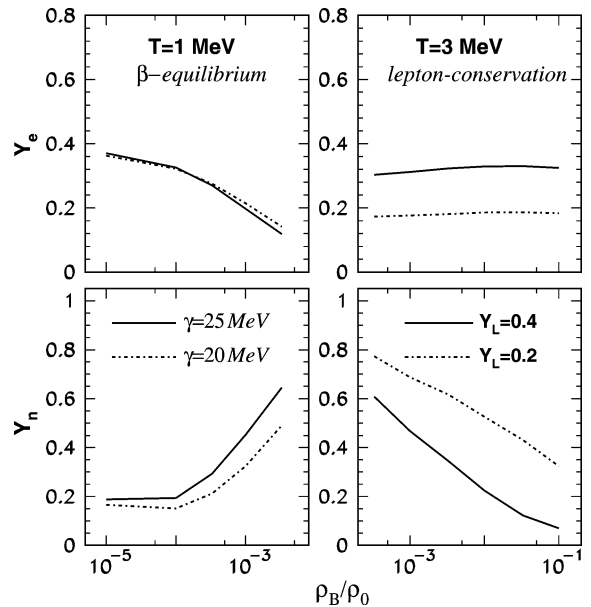


Fig. 3. Average shares of electrons  $Y_e$  (top panels) and free neutrons  $Y_n$  (bottom panels) versus density. Left panels are for the  $\beta$ -equilibrium with  $T = 1$  MeV and different  $\gamma$ . Right panels are for the lepton conservation with  $T = 3$  MeV and different  $Y_L$ .

case the number of free neutrons drops with density reflecting formation of very big nuclei and transition to the liquid phase at  $\rho_B \rightarrow \rho_0$ .

Finally, we find thermodynamic conditions, which allow to produce heavy nuclei in amounts consistent with the solar element abundances. Here we are not pretending to fit the fine structure of these yields, in particular, the pronounced peaks caused by the structure effects of cold nuclei. Our goal is to propose an explanation for the gross distribution of the elements. The results of our fit are presented in Fig. 4. It is interesting that by choosing  $T = 5$  MeV,  $\rho_B = 0.1\rho_0$  and  $Y_L = 0.4$  we are able to achieve a reasonable overall fit. This means that elements heavier than Fe could be produced in proton-neutron stars. However, it is difficult to find a mechanism for ejecting this material from the star. Another possibility is to consider lower densities and temperatures expected in the bubble region. In Fig. 4 we also show the fit with  $T = 1$  MeV and several baryon densities from 0.003 to  $10^{-4}\rho_0$ . In this illustrative calculation we assume that the total baryon number is evenly distributed between the regions with different densities. A better choice would correspond to a temperature and density profile obtained from hy-

<sup>1</sup> An enhancement factor of about 20 is obtained assuming  $E^2$  dependence of the cross section.

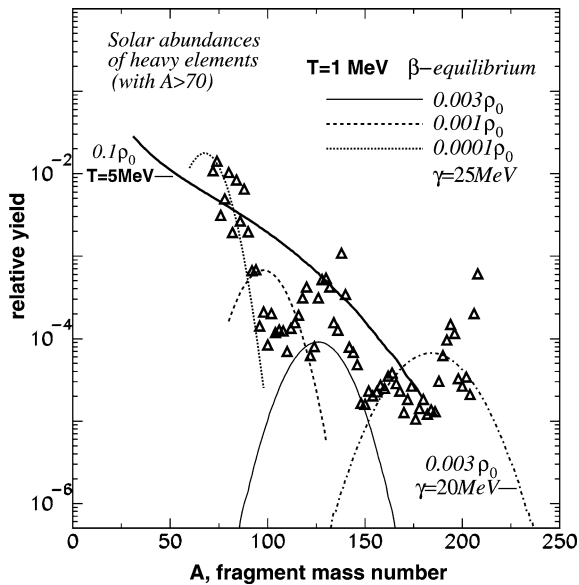


Fig. 4. The mass distribution of heavy elements (with  $A > 70$ ) in solar system. The experimental data (triangles) are taken from [21]. The lines are calculations at densities shown on the figure. The thick solid line is for the lepton conservation at  $Y_L = 0.4$  and  $T = 5$  MeV. The thin solid, dashed, and dotted lines are for the full  $\beta$ -equilibrium, with the standard symmetry energy coefficients  $\gamma$ , and  $T = 1$  MeV; the dot-dashed line is the same but for the reduced  $\gamma$ .

drodynamical simulations of the supernova explosion. As expected [8], during the explosion, dynamical instabilities (convection and other processes) may lead to a large-scale mixing of matter and to large density fluctuations. Appearance of regions with higher density favors production of heavy elements. One can see that we can, in principal, explain the element abundances in this way. Also, a variation of the parameters of hot nuclei, in particular, the  $\gamma$ -coefficient in the symmetry energy, can influence the final predictions.

One should bear in mind that the mass distributions which are presented here correspond to hot primary nuclei. After ejection these nuclei will undergo de-excitation. At typical temperatures considered here ( $T \lesssim 3$  MeV) the internal excitation energies are relatively low, less than 1.0 MeV/nucleon. As well known from calculations [2] and nuclear experiments [5–7], de-excitation of nuclei with  $A \leq 200$  will go mainly by means of the nucleon emission. Then the resulting distributions of cold nuclei are not very different from the primary ones, they are shifted to lower masses by sev-

eral units. One should expect that shell effects (which, however, may be modified by surrounding electrons) will play an important role at the de-excitation stage leading to the fine structure of the mass distribution. We believe that after the de-excitation of hot nuclei, corresponding to the time when the ejected matter reaches very low densities, the  $r$ -process may be responsible for the final redistribution of the element abundances leading to the pronounced peaks around  $A \approx 80, 130$  and  $200$  [21].

In conclusion, we have used statistical approach to study production of hot heavy nuclei during the collapse of massive stars and subsequent supernova explosions. Mass and charge distributions of such nuclei have been calculated under different assumptions regarding temperature, baryon density, electron and lepton composition of the matter. We have demonstrated that this mechanism can contribute significantly to the production of heavy elements in supernova environment and explain gross features of the element abundances. We also expect that the production of hot heavy nuclei may influence the explosion dynamics through both the energy balance and the capture/production of electrons and neutrinos.

## Acknowledgements

This work was supported in part by the Deutsche Forschungsgemeinschaft (DFG) under grant 436 RUS 113/711/0-1, the Russian Fund of Fundamental Research (RFFR) under grant 03-02-04007 and Russian Ministry of Industry, Science and Technology under grant SS-1885.2003.2.1. A.S.B. thanks the Cyclotron Institute of Texas A&M University, Indiana University (Bloomington, IN), and Gesellschaft für Schwerionenforschung (Darmstadt, Germany), where parts of this work were done, for hospitality and support.

## References

- [1] P.J. Siemens, Nature 305 (1983) 410; G. Bertsch, P.J. Siemens, Phys. Lett. B 126 (1983) 9.
- [2] J.P. Bondorf, A.S. Botvina, A.S. Iljinov, I.N. Mishustin, K. Sneppen, Phys. Rep. 257 (1995) 133.
- [3] K.A. Bugaev, M.I. Gorenstein, I.N. Mishustin, Phys. Lett. B 498 (2001) 144.
- [4] A.S. Botvina, et al., Nucl. Phys. A 584 (1995) 737.

- [5] M. D'Agostino, et al., *Nucl. Phys. A* 650 (1999) 329.
- [6] R.P. Scharenberg, et al., *Phys. Rev. C* 64 (2001) 054602.
- [7] S. Hudan, et al., *Phys. Rev. C* 67 (2003) 064613.
- [8] H.-Th. Janka, R. Buras, K. Kifonidis, M. Rampp, T. Plewa, C.L. Fryer (Eds.), Review for 'Core Collapse of Massive Stars', Kluwer Academic Publishers, Dordrecht.
- [9] W.R. Hix, et al., *Phys. Rev. Lett.* 91 (2003) 201102.
- [10] K. Langanke, G. Martinez-Pinedo, *Nucl. Phys. A* 673 (2000) 481.
- [11] C.J. Horowitz, *Phys. Rev. D* 55 (1997) 4577.
- [12] H.A. Bethe, *Rev. Mod. Phys.* 62 (1990) 801.
- [13] A.S. Botvina, A.S. Iljinov, I.N. Mishustin, *Sov. J. Nucl. Phys.* 42 (1985) 712.
- [14] A.V. Ignatiuk, et al., *Phys. Lett. B* 76 (1978) 543.
- [15] M. Prakash, et al., *Phys. Rep.* 280 (1997) 1.
- [16] C. Ishizuka, A. Ohnishi, K. Sumiyoshi, *Nucl. Phys. A* 723 (2003) 517.
- [17] A.S. Botvina, O.V. Lozhkin, W. Trautmann, *Phys. Rev. C* 65 (2002) 044610.
- [18] D.Q. Lamb, J.M. Lattimer, C.J. Pethick, D.G. Ravenhall, *Nucl. Phys. A* 360 (1981) 459; J.M. Lattimer, C.J. Pethick, D.G. Ravenhall, D.Q. Lamb, *Nucl. Phys. A* 432 (1985) 646.
- [19] J.M. Lattimer, F.D. Swesty, *Nucl. Phys. A* 535 (1991) 331.
- [20] A.S. Botvina, I.N. Mishustin, *Phys. Rev. C* 63 (2001) 061601.
- [21] Y.-Z. Quian, *Prog. Part. Nucl. Phys.* 50 (2003) 153.